Direct observation of a band Jahn-Teller effect in the martensitic phase transition of Ni_2MnGa

J. Phys.: Condens. Matter **11** (1999) 4715–4722. Printed in the UK PII: S0953-8984(99)02223-7

Direct observation of a band Jahn–Teller effect in the martensitic phase transition of Ni_2MnGa

P J Brown†‡, A Y Bargawi‡, J Crangle§, K-U Neumann‡ and K R A Ziebeck‡

† Institut Laue-Langevin, BP 156, 38042 Grenoble Cedex 9, France

‡ Department of Physics, Loughborough University, Loughborough LE11 3TU, UK

§ Department of Physics, University of Sheffield, Sheffield S3 7RH, UK

Received 1 March 1999

Abstract. Polarized neutron scattering has been used to determine the changes in the distribution of unpaired electrons which take place in the martensitic transition in Ni_2MnGa. Ni_2MnGa is a ferromagnetic Heusler alloy which undergoes a reversible transition at about 220 K from a high temperature cubic phase to a low temperature tetragonal one. It has been suggested, on the basis of band structure calculations, that the structural phase transition is driven by a band Jahn–Teller distortion involving redistribution of electrons between 3d sub-bands of different symmetries. The results of the neutron scattering experiments show that the transition from the cubic to the tetragonal phase is accompanied by a transfer of magnetic moment from Mn to Ni. The unpaired electrons in the cubic phase have overall e_g symmetry. In the tetragonal phase, the degeneracy of the e_g and t_{2g} bands is raised and the unpaired electrons are redistributed in such a way that the sub-bands based on orbitals extending towards the c-axis are preferentially occupied. Although the experimental moments differ in detail from those expected from band structure calculations, the change in symmetry of the magnetization distribution is consistent with a band Jahn–Teller origin for the phase transition.

1. Introduction

A large number of metallic systems undergo structural martensitic phase transformations which are diffusionless, displacive first order transitions from a high temperature phase to one of lower symmetry below a certain temperature T_m [1]. These transitions, which have been studied for more than a century, are of vital importance because of the product phase in metallurgy and their key role in producing shape memory phenomena. In spite of intense activity, the underlying mechanism giving rise to the transformation is still not well understood and, whilst hysteresis is observed in many properties at T_m, the specific heat anomaly sometimes appears to be of second order. The majority of such transitions have been discussed in terms of soft mode behaviour in which the frequency of a particular low lying phonon branch varies as $\omega^2 = a(T - T_m)$ producing a lattice distortion stabilized by higher order non-linear contributions to the free energy [2]. However, whilst a dip in the phonon dispersion, at a wave vector corresponding to the periodicity of the closed-packed planes in the martensitic phase, is often observed, the softening is incomplete. Consequently, the soft mode model has only been found to be appropriate for a very limited number of the known martensitic transitions [3]. The discovery of precursor effects above T_m has led to other models being proposed in which nucleation processes give rise to two length and time scales: one associated with atomic and the other with mesoscopic phenomena [4, 5]. In this paper, new results obtained on the shape memory compound Ni_2MnGa are presented which pertain to the atomic length scale. Results, obtained

0953-8984/99/244715+08$19.50

on the same compound, which address the mesoscopic behaviour of the transition will be published separately.

Ni_2MnGa is one of a group of shape memory effect compounds which is currently exciting considerable interest since it is one of the very few which are also ferromagnetic. The origin of the shape memory effect in Ni_2MnGa is in the martensitic transition which takes place on cooling through 200 K from the cubic $L2_1$ Heusler structure to a tetragonal phase. The transformation can be described as a simple contraction along one of the [100] directions of the cubic phase without any change in atomic positions. There is a strong deformation of the cell ($c/a = 0.94$) but a reduction of only $\approx$1% in cell volume [6]. This phase transition is remarkable in that, in spite of a strong deformation of the unit cell, it is reversible and a single crystal can be cycled through it many times without breaking. The phase transition has been extensively investigated particularly by inelastic neutron scattering, which reveals the presence of precursor effects above T_m and an incomplete softening of the TA2 phonon mode at a wave vector q of 0.33 reciporocal latttice units [7]. These observations have been correlated with a softening of certain elastic constants [8] particularly c' which is $\frac{1}{2}(c_{11} - c_{12})$ and is determined by the initial slope of the TA2 phonon propagating in the [110] direction.

Below 378 K, Ni_2MnGa orders ferromagnetically. The cubic and tetragonal phases have different magnetic anisotropy; their magnetizations differ in weak fields but converge for fields greater than 2 T. The saturation magnetization at low temperatures is 4.12 μ_B per Ni_2MnGa formula unit. Ultrasonic measurements carried out in a magnetic field at room temperature reveal a strong dependence of the elastic constants, especially c' on applied field [9]. These results suggest that the pre-martensitic transition may be driven by magneto-elastic interactions. The conduction electron concentration is known to be a predominant factor in characterizing the structural and magnetic properties of Heusler alloys [10] and it has also been invoked to account for the phase transition in Ni_2MnGa [7]. However, similar phase transitions in other Heusler alloys (Rh_2CoSn) [11] have been ascribed to a band Jahn–Teller mechanism originally proposed to account for the structural phase transitions observed in A15 compounds [12]. In this model, the lattice distortion breaks the degeneracy of the d bands in the vicinity of the Fermi level, thus causing a redistribution of electrons in these bands with a consequent reduction of the free energy. More recently, the results of band structure calculations have have been used to argue that in Ni_2MnGa also, the structural phase transition is driven by a band Jahn–Teller distortion [13]. Since Ni_2MnGa is ferromagnetic, a detailed investigation of the spin density distribution above and below the transition can be carried out using polarized neutrons. In this way, any re-population of electrons can be quantified and the appropriateness of the band Jahn–Teller mechanism assessed.

2. Material

Using starting elements of 4N purity, a single crystal of Ni_2MnGa was pulled from the melt using a cold crucible tri-arc furnace designed and built in the Department of Physics at Loughborough University. The crystal was of cylindrical shape with diameter 2 mm and length 7 mm. Subsequent neutron Laue photographs confirmed the sample to be single with a $[1\bar{1}0]$ direction parallel to the axis of the cylinder.

3. Bulk properties

Magnetization measurements were carried out between 2 and 300 K using a squid magnetometer in which fields of up to 5 T could be applied parallel to the $[1\bar{1}0]$ axis of

the crystal. The magnetization in a field of 4.6 T was 3.39 μ_B per formula unit at 100 K and 2.79 μ_B at 230 K. In high fields the magnetization, shown in figure 1, exhibits a small but distinct anomaly which occurs at ≈220 K on heating. The anomaly, which is more pronounced in lower fields, arises from the change in magnetic anisotropy associated with the structural phase transition. It is also clearly shown in specific heat measurements made, using a modified adiabatic heat pulse calorimeter, on a specimen cut from the same boule as the single crystal. The heat capacity measurements are displayed in the inset of figure 1; the shape of the anomaly is of the *lambda* type often observed in martensitic phase transitions [14]. Neutron diffraction measurements in zero field, made on the same crystal for which the magnetization was measured, show that on heating, the transition from the tetragonal to the cubic phase starts at 200 K and is complete by 220 K.

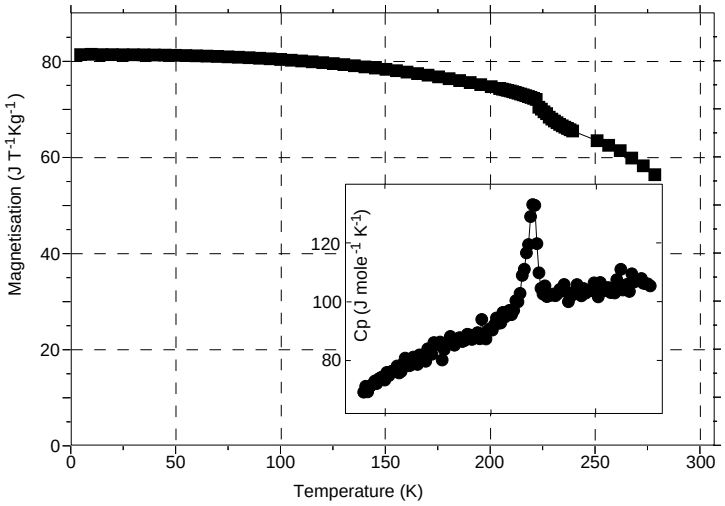

Figure 1. Magnetization of Ni_2MnGa at 4.6 T plotted as a function of temperature. The inset shows the temperature variation of the specific heat in the vicinity of the phase transition.

4. Neutron diffraction measurements

4.1. Integrated intensity measurements

Measurements of the integrated intensities of all reflections with $\sin\theta/\lambda < 0.8$ Å^{-1} were made on the diffractometer D9 at ILL Grenoble at a wavelength of 0.84 Å. The crystal was maintained at 230 K using a two stage Displex refrigerator mounted on the χ circle of the Eulerian cradle. The intensities of equivalent reflections were averaged together and a mean observed structure amplitude for each set of equivalents was calculated. The agreement between equivalent reflections was good, leading to a merging R factor of 1.8% on F^2.

4.2. Polarized neutron measurements

Polarized neutron flipping ratio measurements were carried out using the polarized neutron diffractometer D3 located on the hot source at ILL Grenoble. The crystal was mounted initially with its $[1\bar{1}0]$ axis vertical inside a superconducting magnet located on the omega table of the diffractometer. On cooling through the phase transition the cubic (220) reflection split into two reflections separated by the angle ν (the inclination of the detector) one above and one

below the cubic position. This shows that only two of the three possible tetragonal domains are present: those whose tetragonal *c*-axes are parallel to the cubic [100] and [010] axes. The domain whose *c*-axis would have been perpendicular to the long axis of the crystal, and hence to the field direction, was not formed. With this arrangement of domains, it was not possible to measure a significant number of the groups of reflections which are equivalent under cubic symmetry but distinct in the tetragonal phase. In an attempt to change the domain population the crystal was demagnetized by heating it above T_c and cooling in zero field. Its previous finite remanence disappeared but there was no apparent change in domain population. The crystal was subsequently mounted with its long axis horizontal and a [113] axis parallel to the field. In this orientation a reasonable fraction of the full set of reflections for one domain of the tetragonal phase was accessible. Flipping ratios were measured with $\lambda = 0.84$ Å, for all reflections in the cubic phase at $T = 230$ K and for all accessible reflections in one domain of the tetragonal phase at $T = 100$ K, with $\sin\theta/\lambda < 0.64$ Å^{-1}. A set of strong reflections was measured at the shorter wavelength $\lambda = 0.42$ Å at both temperatures to check for extinction.

5. Analysis of the data

5.1. Integrated intensities

Crystallographic data for Ni_2MnGa are given in table 1. The three independent sites, A, B, C of the Heusler alloy structure, are ideally occupied by Mn, Ga and Ni respectively. The structure amplitudes obtained from the integrated intensity measurements were used in a least squares refinement to establish the degree of chemical order and the extinction properties of the crystal. An initial refinement in which the occupancy of the B site by Ga was fixed to unity gave rise to a site scattering length for the C site slightly greater than that of Ni. Since Ni has a larger scattering length than either Mn or Ga this was taken to indicate that the C site was fully occupied by Ni. With this assumption, and that of full occupancy of all sites, the results shown in table 1 were obtained. These give evidence for some disorder between the Mn and Ga atoms and an overall Mn deficit of some 15(1)%. Scattering lengths of −1.67, 6.96 and 10.3 fm for the A, B and C sites, respectively, were used in the subsequent analysis of the polarized neutron data. Introducing a parameter to model extinction did not give any improvement in the goodness of fit.

Table 1. Crystallographic data for Ni_2MnGa at 230 K.

Space group $Fm3m$	$a = 5.825$ Å		
	A (Mn)	4a	000
Atomic positions	B (Ga)	4b	$\frac{1}{2}\frac{1}{2}\frac{1}{2}$
	C (Ni)	8c	$\frac{1}{4}\frac{1}{4}\frac{1}{4}$
Parameters of least squares refinement	A	B	C
Site scattering length (fm)	−1.67(14)	6.96(4)	10.3†
Element scattering length (fm)	−3.73	7.30	10.3
Mn occupancy	0.81(7)	0.03(1)	0
Ga occupancy	0.19(2)	0.97(1)	1
Ni occupancy	0	1	0
Magnetic moments (μ_B)	2.3†	0†	0.22†
Isotropic temperature factors (Å^2)	1.05(20)	1.02(4)	1.22(3)
R factor on F	3.1%		

† Parameter fixed in the refinement.

5.2. Polarized neutron flipping ratios

The observed flipping ratios were used to calculate the ratios γ, of the magnetic to nuclear structure factors, taking into account the degree of polarization of the neutron beam in the two spin states. The γs of equivalent reflections within each set of measurements were averaged together. The agreement between the γs of the same reflections measured at the two different wavelengths was rather good indicating, in agreement with the integrated intensity measurements, that the effects of extinction can be neglected. The data taken with the two different crystal orientations were merged together and the γ values multiplied by the calculated nuclear structure factors to give two sets of magnetic structure factors one for $T = 230$ K which was averaged using cubic symmetry, and the other for 100 K, averaged according to tetragonal symmetry.

5.3. Least squares fits to the magnetic structure factors

A first fit to the magnetic structure factors was carried out using a model in which all the magnetization is associated with the A and C sites and has a distribution given by the Mn^{2+} and Ni^{2+} spherical free atom form factors, respectively. The least squares fit of this model gave moments of 2.36(2) and 0.25(2) μ_B for the A and C sites, respectively, at 230 K, and 2.84(2) and 0.38(1) μ_B at 100 K. Allowing a moment also on the B site (modelled with the Mn^{2+} form factor) improved the goodness of fit by a factor of more than 2 and indicated a small negative value of $\approx -0.1\mu_B$ for the moment at the B site at both temperatures. The B site scattering length indicated about 3% occupancy by Mn which would lead to $\approx -3.3\mu_B$ per Mn atom in the B sites.

Even when moments on all three sites are included, significant differences remain between the observed and calculated structure factors which may be due to non-validity of the assumption of spherical symmetry in the model. The d orbitals which the magnetic electrons are presumed to occupy are split by a cubic crystal field into a doubly degenerate e_g and a triply degenerate t_{2g} set which have different spatial distributions. The tetragonal distortion splits these orbitals further leading to 1 doubly and 3 singly degenerate sets. The 2 singly degenerate sets x^2–y^2 and $3z^2$–r^2 are derived from the cubic e_g orbitals and the singly degenerate xy and doubly degenerate $xz \pm yz$ sets from the t_{2g} orbitals. The model was extended to allow unequal occupation of these different orbitals and a least squares fit of their occupancies on the A and C sites effected. For the 230 K data, allowing such an aspherical moment distribution gave no significant change in the goodness of fit, whereas for the 100 K data there was a marked improvement. The quantitative results of all the least squares fits are summarized in table 2. They show that in the cubic phase all the e_g and t_{2g} orbitals are almost equally occupied leading to overall e_g symmetry. In the tetragonal phase there is a significant depletion of the xy member of the t_{2g} set at the A site. At the C site there is a transfer of unpaired spin to the $3z^2$–r^2 member of the e_g set and depletion of the $xz \pm yz$ member of the t_{2g} set.

5.4. Reconstruction of the magnetization distribution

The results of the previous subsection suggest that a significant redistribution of the magnetization takes place in the cubic to tetragonal transformation and it is interesting to see to what extent the results obtained by model fitting can be substantiated by a model-free analysis of the data. Such a model-free analysis can be obtained by reconstructing a magnetization distribution which would predict the observed magnetic structure factors exactly. Such a distribution is given by the Fourier transform of the magnetic structure factors. However it is not unique since only a limited set of data, measured with only limited accuracy is available.

Table 2. Least squares fits to the magnetic structure factors of Ni_2MnGa at 230 and 100 K.

	$T = 230$ K				$T = 100$ K		
Site	A (Mn)	B (Ga)	C (Ni)		A (Mn)	B (Ga)	C (Ni)
Moment (μ_B)	2.30(1)	0†	0.22(6)		2.84(2)	0†	0.38(1)
‡χ^2		142				32	
Moment (μ_B)	2.27(2)	−0.12(2)	0.19(2)		2.82(1)	−0.08(1)	0.367(7)
‡χ^2		20				13	
Moment (μ_B)	2.29(3)	−0.11(3)	0.20(2)		2.80(1)	−0.06(1)	0.358(8)
e_g(%)	51(1)		58(8)	x^2–y^2(%)	23(2)		15(12)
				$3z^2$–r^2(%)	20(2)		48(9)
t_{2g}(%)	49(1)		42(8)	xy(%)	13(2)		27(12)
				$zx \pm zy$(%)	44(2)		9(13)
‡χ^2		20				9	

†Parameter fixed in the refinement.
‡The large difference between the χ^2 values for the 230 and 100 K data is due to the relatively greater statistical precision of the magnetic structure factors measured for the cubic phase.

The problem of how to construct the best distribution from the available data, given any *a priori* assumption about the form of that distribution, has been tackled using the concept of maximum entropy [15, 16]. The usual *a priori* assumption is that the distribution is flat, and this is clearly not applicable to the magnetization in a crystal which is known to be concentrated around the atomic sites. In the present case, however, the object of the experiment is to observe the redistribution of the magnetization which accompanies the cubic to tetragonal transition. If the data which are used in the reconstruction are the differences between the magnetic structure factors for the same reflections, measured above and below the transition and normalized to the same total moment, then the reconstructed density should correspond to just this redistributed magnetization. A flat density, close to zero, is then a reasonable *a priori* assumption. Figure 2 shows a section through the origin parallel to $[1\bar{1}0]$ of this density. There is negative density at the A (Mn) site and positive density at the C (Ni) and B (Ga) sites indicating that magnetization is transferred from Mn to Ni in the transition. The negative density at the A site is extended along the [110] direction, which is consistent with the depletion of the xy d-orbitals. The positive density at the C site is elongated along z, consistent with the increase in the number of unpaired electrons in the $3z^2$–r^2 orbitals.

An alternative *a priori* density is the cubic average of the tetragonal magnetization. Any deviations from this average should be real features corresponding to deviations from cubic symmetry. Figure 3 shows the $[1\bar{1}0]$ section of this tetragonal deformation density. It shows the repopulation of the $xz \pm yz$ at the expense of the xy t_{2g} orbitals on the Mn atoms rather more clearly than figure 2 and is equally clear in showing the increase in the number of unpaired electrons in the $3z^2$–r^2 orbitals on Ni.

6. Discussion

The most significant changes, which take place in the distribution of magnetization at the cubic to tetragonal phase transition, are an increase in the magnetic moment of nickel relative to that of manganese and a redistribution of magnetization amongst the orbitals whose degeneracy is broken by the lowered symmetry. Those which involve the z-coordinate become predominant. Since the magnetization (figure 1) varies relatively smoothly with temperature the increase in the ratio of the nickel to manganese moments most probably results from transfer of electrons from the nearly full 3d band of nickel to a more than half-filled 3d band of manganese.

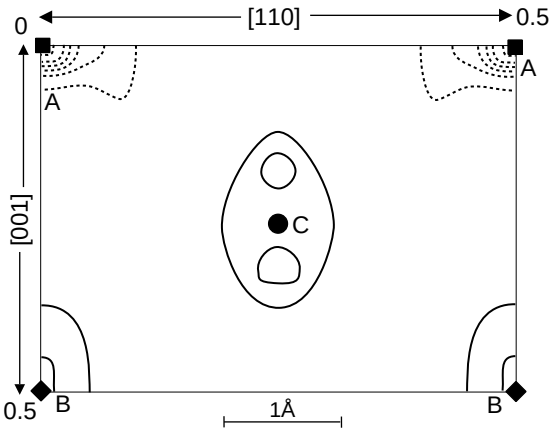

Figure 2. Maximum entropy reconstruction of the redistribution of magnetization which takes place in the cubic to tetragonal transformation. The map shows the section ‖ to [110] passing through the origin.The contour intervals are 0.125 μ_B Å^{-3} negative contours are shown as dashed lines.

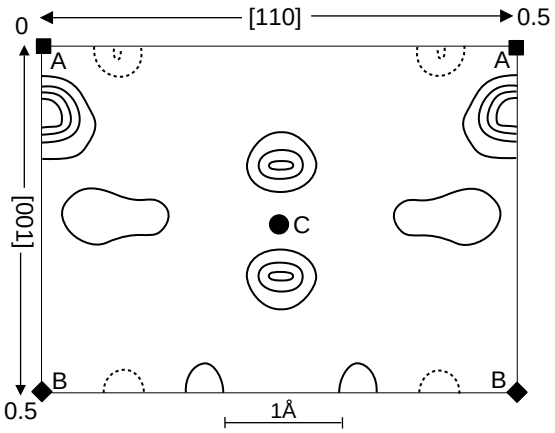

Figure 3. Maximum entropy reconstruction of the tetragonal components of the magnetization distribution in Ni_2MnGa at 100 K. The map shows the same section as figure 2. The contour intervals are 0.05 μ_B Å^{-3}.

In a normal Jahn–Teller transition such as that associated with Cu^{2+} or Mn^{3+} ions the splitting of degenerate energy levels which couple to thermal vibrations drive the transition. In the band Jahn–Teller mechanism it is the splitting of energy sub-bands which are degenerate in the high temperature phase which enables the electrons to redistribute themselves so as to lower the free energy. In the band model there is an increase in the width of the energy bands because, when the crystal deforms there is a change in the degree of overlap of the associated orbitals. Since, in the tetragonal phase of Ni_2MnGa $c/a < 1$, the bands associated with orbitals directed along c will be broader than those associated with orbitals in the a–b plane. Specifically for 3d electrons the $3z^2$–r^2 component of the sub-band will broaden and the x^2–y^2 component will narrow. For the t_{2g} sub-band the doubly degenerate $xz \pm yz$ component will broaden and the xy component become narrower. The redistribution of magnetization found in the experiment supports this Jahn–Teller band mechanism, in that the $xz \pm yz$ and $3z^2$–r^2 components of the sub-bands are populated at the expense of the xy and x^2–y^2 components.

The fact that it is the e_g sub-band which shows the effect at the C site, and the t_{2g} sub-band at the A site, must be due to the details of the band structure.

The band structure of Ni_2MnGa has been calculated by [13], and has been used by them to obtain the site magnetic moments in the cubic and tetragonal phases. They find for the cubic phase: Ni 0.29, Mn 3.41 and Ga $-0.05\ \mu_B$ and for the tetragonal phase Ni 0.24, Mn 3.41 and Ga $-0.05\ \mu_B$, at a calculation temperature of 0 K. The experimental values normalized to 0 K, using the magnetization curve of figure 1 are Ni 0.24, Mn 2.74 and Ga $-0.013\ \mu_B$ in the cubic phase, and Ni 0.36, Mn 2.83 and Ga $-0.06\ \mu_B$ in the tetragonal phase. Thus, not only do the experimental results contradict the calculation in giving a higher total transition metal moment in the tetragonal phase, but they also suggest a small redistribution of moment (2%) in favour of manganese in the tetragonal phase, whereas in the experiment the redistribution is in favour of nickel (6%). The composition of the bands which are active at the Fermi surface are not identified in the DOS curves in [13] but following the suggestion of [17] they can be assigned by comparison with previous calculations on similar Heusler alloys containing cobalt instead of Ni [18]. With this identification the Fermi level lies just above a peak in the DOS of the minority spin Ni e_g band and at a position in the Mn band at which there is an almost equal DOS of majority and minority spin t_{2g} states. The peak in the minority spin Ni e_g band is lowered and broadened in the cubic to tetragonal transition, whereas there is little change in the Mn bands near the Fermi surface. The experimental results are consistent with depletion of the minority spins in the Ni e_g band, assuming the higher energy ones are derived from antibonding $3z^2{-}r^2$ orbitals. They also suggest that the extra electrons are accommodated in minority spin states of xy character in the Mn band.

Acknowledgments

The authors are grateful to B Dennis and J W Taylor for experimental help with the magnetization and specific heat measurements. They also wish to thank Professor S Ishida for providing details of his band structure calculations not available in the published papers.

References

[1] Christian J W 1965 *Theory of Phase Transitions in Metals and Alloys* (Oxford: Pergamon)
[2] Cochran W 1960 *Adv. Phys.* **9** 387
[3] Anderson P W 1960 *Fizika Dielectrikov* ed G I Skanavi (Mosocw: Acad. Nauk. SSR)
[4] Krumhansl J A and Gooding R J 1989 *Phys. Rev.* B **39** 3047
[5] de Gennes P G 1973 *Fluctuations, Instabilities and Phase Transitions* ed T Riste (New York: Plenum)
[6] Webster P J, Ziebeck K R A, Town S L and Peak M S 1984 *Phil. Mag.* B **49** 295
[7] Zheludev A, Shapiro S M, Wochner P, Schwartz A, Wall M and Tanner L E 1995 *Phys. Rev.* B **51** 11 310
[8] Manosa L, Gonzalez-Comas A, Obrado E, Planes A, Cherenko V A, Korkin V V and Cesari E 1997 *Phys. Rev.* B **55** 11 068
[9] Planes A, Obrado E, Gonzales-Comas A and Manosa L 1997 *Phys. Rev. Lett.* **79** 3926
[10] Jassim I K, Neumann K-U, Visser D, Webster P J and Ziebeck K R A 1992 *J. Magn. Magn. Mater.* **104–107** 2072
[11] Suits J 1976 *Solid State Commun.* **18** 423
[12] Labbé J and Friedel J J 1966 *Phys. Radium* **27** 153 and 303
[13] Fujii S, Ishida S and Asano S 1987 *J. Phys. Soc. Japan* **58** 3657
[14] Parsons M J, Brown P J, Crangle J, Neumann K-U, Ouladdiaf B, Smith T J, Zayer M K and Ziebeck K R A 1998 *J. Phys.: Condens. Matter* **10** 8523
[15] Gull S F and Daniell G J 1978 *Nature* **272** 686
[16] Papoular R J and Gillon B 1990 *Europhys. Lett.* **13** 229
[17] Ishida S 1999 Private communication
[18] Ishida S, Akazawa S, Kubo Y and Ishida J 1982 *J. Phys. F: Met. Phys.* **12** 1111